

Water Extract of Sporoderm-Broken Spores of *Ganoderma lucidum* Induces Osteosarcoma Apoptosis and Restricts Autophagic Flux

This article was published in the following Dove Press journal:
OncoTargets and Therapy

Wenkan Zhang^{1,2,*}
Zhong Lei^{1,2,*}
Jiahong Meng^{1,2,*}
Guoqi Li^{1,2}
Yuxiang Zhang^{1,2}
Jiaming He^{1,2}
Weiqi Yan^{1,2}

¹Department of Orthopedics Research Institute, The Second Affiliated Hospital, Zhejiang University School of Medicine, Hangzhou, Zhejiang 310009, People's Republic of China; ²Department of Orthopedic Surgery, The Second Affiliated Hospital, Zhejiang University School of Medicine, Hangzhou, Zhejiang 310009, People's Republic of China

*These authors contributed equally to this work

Purpose: Osteosarcoma (OS) is a malignant bone tumor with easy metastasis and poor prognosis. *Ganoderma lucidum* (*G. lucidum*), a traditional Chinese medicine, was reported playing a critical role in suppressing multiple tumor progress. So we wanted to investigate the effects and molecular mechanisms of water extract of sporoderm-broken spores of *G. lucidum* (BSGLWE) on osteosarcoma.

Methods: In vitro, the effects on cell proliferation of BSGLWE in osteosarcoma cells were detected by CCK-8, colony formation assay and flow cytometry; migration ability of osteosarcoma cells was evaluated by cell scratch and transwell assays. Cell apoptosis and autophagy were tested by transmission electron microscopy (TEM). Potential signaling pathways were detected by Western blotting and immunofluorescence. In xenograft orthotopic model, the luminescence intensity measured by an in vivo bioluminescence imaging system, and the expression of related proteins in tumor cells were assessed by IHC analysis.

Results: BSGLWE suppressed the proliferation and migration of osteosarcoma cells in a dose-dependent manner, and osteosarcoma cell cycle progression at the G2/M phase was arrested by the BSGLWE. In addition, increased apoptosis-related protein expression meant BSGLWE induced caspase-dependent apoptosis of osteosarcoma cells. TEM results indicated that BSGLWE promoted the formation of apoptotic bodies and autophagosomes in HOS and U2 cells. Western blotting or immunofluorescence and rescue assay revealed that BSGLWE blocked autophagic flux by inducing initiation of autophagy and increasing autophagosome accumulation of osteosarcoma cells. BSGLWE not only repressed the angiogenesis in the mouse model, but also induced apoptosis and blocked autophagy in vivo.

Conclusion: BSGLWE inhibits osteosarcoma progression.

Keywords: osteosarcoma, sporoderm-broken spores of *Ganoderma lucidum* water extract, cancer therapy, apoptosis, autophagy

Introduction

Osteosarcoma (OS) is the most common type of malignant bone tumor, which basically occurs in children and adolescents. Osteosarcoma usually emerges in the metaphyseal end of the long tubular bone, most commonly at the femur and the tibia near the knee.¹ Because of its rapid development and early metastasis, the 5-year survival rate of the patients is unsatisfactory.² Chemotherapy combined with surgical treatment is still the main treatment for osteosarcoma. However, drug-induced side effects and tumor recurrence after surgery reduce patient quality of life and cut down the patient survival rate.³ Therefore, finding a suitable drug that has less side effects and higher potency is inevitable.

Correspondence: Weiqi Yan
Department of Orthopedic Surgery,
The Second Affiliated Hospital, Zhejiang
University School of Medicine, #88
Jiefang Road, Hangzhou, Zhejiang 310009,
People's Republic of China
Email wyan@zju.edu.cn

Ganoderma (G) lucidum, also named as “*Lingzhi*” in China and “*Rei-Shi*” in Japan, is one of the widely accepted traditional Chinese medicines among eastern countries for more than 2000 years. In the past few decades, *G. lucidum* was found that it is an effective supplemental medicine to prevent and treat various diseases. In addition, recent studies in the last decade revealed that *G. lucidum* has a large amount of pharmacological functions, such as immunity enhancement, anti-oxidative, anti-inflammatory and antitumor effects.⁴⁻⁶ It is reported that *Ganoderma lucidum* polysaccharides (GLPs) is one of the main effective components isolated from *G. lucidum*, which not only inhibit diverse cell migration and invasion but also suppress tumor progress in different tumor cell-bearing mice.^{7,8} Many studies showed GLPs might serve as a practicable anticancer drug in the treatment of many kinds of tumors, such as melanoma, lung cancer, breast cancer, endometrial cancer, bladder cancer and colorectal cancer.^{7,9,10} Water or ethanol extract of sporoderm-broken spores of *Ganoderma lucidum* (BSGLWE or BSGLEE), which generally consists of GLPs, inhibits colorectal cancer carcinogenesis through acceleration of apoptosis, promotion of cell cycle arrest and reducing genes responsible for cell proliferation.^{9,11}

Autophagy is the process that those aging or damaged organelles are surrounded by the endoplasmic reticulum, and the generated vesicles are called autophagosomes, which fuse with lysosomes and form autolysosomes to conduct degradation.¹² Autophagy is usually triggered by many stimuli that ultimately lead to cell death, and it is involved in many physiological and pathological changes that mediated by a number of autophagy-related proteins. The function of autophagy is regarded as preventing the accumulation of damaged cell fragments and helping the body maintain homeostasis.¹³ Apoptosis, a classic mechanism of inducing cell death, involves a series of morphological changes, which leads to the formation of apoptotic bodies. Autophagy is normally considered as a protective response to stress, because autophagy reduces the tendency of cells to undergo apoptosis.^{14,15} However, many reports indicated that autophagy has the opposite effects on apoptosis: autophagy facilitates the activation of apoptosis.^{16,17} We did this study to figure out whether BSGLWE can inhibit osteosarcoma by regulating the level of apoptosis and autophagy.

In the current study, we examined the effects of BSGLWE on osteosarcoma cells in vitro and in vivo and revealed that BSGLWE had antitumor potential against

osteosarcoma. We further investigated the underlying mechanisms, and the results suggested that BSGLWE induced apoptosis and restricted autophagic flux in osteosarcoma both in vitro and in vivo.

Materials and Methods

Cell Culture and Reagents

The human osteosarcoma cell lines MNNG/HOS (HOS) (CRL-1547TM, ATCC), U2-OS (U2) (HTB-96TM, ATCC) and MG63 (CRL-1427TM, ATCC) were purchased from the Cell Bank of the Chinese Academy of Sciences (Shanghai, China). HOS and MG63 cells were cultured in Dulbecco's modified Eagle's medium (DMEM), and U2 in RPMI 1640. Both media included 10% fetal bovine serum (FBS) and 100 U/mL penicillin and 100 ug/mL streptomycin. The cells were incubated at 37°C in an environment with 5% CO₂, then were harvested and subcultured upon reaching 80–90% confluence. 3-methyladenine (3-MA) was obtained from Beyotime Biotechnologies (Jiangsu, China), and chloroquine (CQ) was purchased from MedChemExpress Technology (New Jersey, USA).

Preparation of BSGLWE

The Shouxiangu^R wall-broken *Ganoderma lucidum* spores (BSGL) were provided by Jinhua Shouxiangu Pharmaceutical Co. Ltd (Zhejiang, China). Hot water extraction method is our way to extract the polysaccharides from the BSGL. In simple terms, 2 g of BSGL was placed in 10 mL of double-distilled water, and stirred (250 rpm) at 70°C for 12 hrs in a water bath. The solution was centrifuged at 1500 rpm for 10 mins to aspirate supernatant, which was concentrated and freeze-dried using a freeze dryer (LABCONCO, USA). For subsequent experiments in vitro, the powder of sporoderm-broken spores of *Ganoderma lucidum* water extract (BSGLWE) was dissolved in DMEM with 10% FBS as a 50 mg/mL stock solution, and then passed through a 0.22-μm filter to remove bacterium.

Cell Proliferation Assays

To test the inhibitory effects of BSGLWE on osteosarcoma cells, a CCK8 Kit (Dojindo Laboratories, Kumamoto, Japan) was used to detect cell viability. Based on the manufacturer's instruction, cells were, respectively, seeded into a 96-well plate approximately 5×10³ cells per well. After the cells were adherent to the bottom of the well, we replaced the medium to make the cells are treated with

various concentrations of BSGLWE (0–16 mg/mL) for different periods of time (0–72 hrs). In order to explore the underlying mechanisms, cells were treated with different concentrations of BSGLWE and co-incubated with 3-MA (3mM) for 24 hrs. Then, CCK8 reagent (10 uL) was added to each well, after incubation for 2–4 hrs, the absorbance was measured using an MR7000 microplate reader (Dynatech, NV, USA) at 450 nm daily for 3 days. Colony formation was used to assess the cell proliferation activity. Cells in the exponential growth phase were plated into 6-well plates and allowed to adhere. The HOS and U2 cell densities were 1,000 and 500 cells per well, respectively. The cells were treated with control medium or different concentrations of BSGLWE for 12–18 days. The colonies were washed three times with 1× phosphate-buffered saline (PBS), fixed with paraformaldehyde about 15–20 mins and stained with 0.1% crystal violet (Beyotime); next, they were visualized under a microscope and photographed. The number of colonies (>50 cells/colony) was counted.

Cell Cycle Flow Cytometry Assay

$2-3 \times 10^5$ cells were seeded in a 6-well plate per well and incubated with different concentrations of BSGLWE (0, 4, 6, 8 mg/mL) for 24 hrs. Then, the cells were washed with PBS and collected. Afterward, the cells were fixed in 75% ice-cold ethanol, and storage at -20°C for at least 2 hrs. Cells were hydrated with PBS for 15 mins after being centrifuged for 5 mins at 1200 rpm and aspirate the supernatant. Then, the cells were centrifuged and stained with PI (50 $\mu\text{g/mL}$; MultiSciences Zhejiang, China) for 30 mins. Samples were subsequently analyzed by flow cytometer (Becton–Dickinson NewJersey, USA).

Cell Migration Assays

The migration capabilities of HOS and U2 cells were detected using a wound-healing assay. When the cell proliferation reached about 90% confluence, we utilized a 10 uL pipette tip to scratch the cell layer stably to make a wound line. After that, the cells were washed softly for 3 times with PBS to remove debris. A serum-free medium was added before cells were photographed under a microscope immediately. Then, cells were cultured with treatment medium (control group, 2 mg/mL BSGLWE group, 4 mg/mL BSGLWE group) for 12 h. At that time, the pictures of the cells were photographed again. The wound area was analyzed using the software ImageJ.

Transwell chambers (with 8 μm -pore-sized membranes, Corning Life Science, USA) were used to further assess the cell migration abilities. The chambers were washed with serum-free medium, after which 600 uL treatment medium (control group, 2 mg/mL BSGLWE group, 4 mg/mL BSGLWE group) containing 10% FBS was added in the lower chamber, respectively, while cells (200 μL ; 10^6 cells/mL) were planted in the upper chamber. After 8 h of incubation, the chambers were fixed with 4% paraformaldehyde for 15–20 mins and subsequently stained with 0.1% crystal violet for 15 mins. Then, the cells were wiped off the upper membrane, and those lower membrane cells were counted and taken photos by inverted microscopy.

Transmission Electron Microscopy Detection

Transmission electron microscopy is a commonly used means of observing cellular ultrastructure. Apoptotic bodies and nuclear condensation can be observed by TEM during cell apoptosis. Cells treated with BSGLWE (4mg/mL) were first fixed with 2.5% glutaraldehyde and fixed again with 1% osmium tetroxide. Cells were embedded in Epon after dehydrated with different concentrations of alcohol (30–100%). Ultrathin sections (70–90 nm) were generated for observation under a transmission electron microscope.

Apoptosis Measurement

Apoptosis was calculated using the reagent Annexin V-APC/7-aminoactinomycin D (7-AAD; Multi-Sciences, Hangzhou, Zhejiang, China). Cells were seeded into a six-well plate at a density of approximately $2-3 \times 10^5$ cells per well and treated with different concentrations of BSGLWE for 24 hrs. Then, the cells were harvested with trypsin and pelleted by centrifugation. After being washed 3 times with PBS, the cells were incubated with Annexin V-APC/7-AAD kit for 15 min at normal temperature in the dark. All procedures followed the manufacturer's protocols. Then, the samples were measured and analyzed by a flow cytometer (FACSCalibur, BD, San Jose, CA, USA). Annexin V-APC (+)/PI (–) and Annexin V- APC(+)/PI(+) staining signified cells that were in the early and later stages of apoptosis, respectively.

The Hoechst 33342 nuclear staining method was used to measure morphological changes in apoptotic cells. First, 4×10^5 cells per well were seeded into a six-well plate and treated with different concentrations of BSGLWE for 24

hrs, then cells were cultured with Hoechst 33342 for approximately 15 mins. At last, a fluorescence microscope (Olympus, Tokyo, Japan) was equipped to visualize morphological changes of apoptotic cells at 365 nm.

Western Blot Assays

Cells were treated with different concentrations of BSGLWE (0, 4, 6, 8 mg/mL) for 24 hrs. In order to explore potential mechanisms, cells were planted into a six-well plate, and then treated with different concentrations of BSGLWE (0, 4, 8mg/mL) in the presence or absence of 3-MA (3mM) or CQ (8uM). After being collected, the cells were lysed with RIPA buffer (Sigma-Aldrich, St. Louis, MO, USA), which included protease inhibitor and phosphatase inhibitor cocktail (Sigma-Aldrich). According to the steps in the manufacturer's protocols, the supernatant was collected. A BCA protein assay kit (Beyotime) was used to quantify the total amount of protein. The equal amounts of protein samples were separated by 8–15% SDS-PAGE at 75 V for 1.5 hrs and subsequently transferred onto 2.2 um polyvinylidene fluoride membranes (Millipore, Billerica, MA, USA) at 250 mA for 2 hrs in a humid atmosphere. The membranes were blocked with 10% milk or 5% bovine serum albumin (BSA; Sigma-Aldrich) and incubated with the primary antibody overnight at 4°C. After being washed with TBST for 3 times, 10 mins each time, the membranes were incubated with horseradish peroxidase(HRP)-conjugated secondary antibodies (Huabio, Hangzhou, Zhejiang, China) for 1 hr at room temperature. The target bands were observed and development using an enhanced chemiluminescence kit (Millipore). The details for the primary antibodies are as follows: Bcl-2 (1:2000, Cat: ab182858, ABCAM, MA, USA), Bcl-xl (1:1000, Cat: 2764S, Cell Signaling Technology, Beverly, MA, USA), Apoptosis antibody sample kit (1:1000, Cat: 9915T, CST), LC3B (1:1000, Cat: 3868S, CST), ATG5(1:2000, Cat: ET1611-38, Huabio), ATG12 (1:800, Cat: M1701-4, Huabio), p62 (1:800, Cat: EM0704, Huabio). The secondary antibodies were as follows: goat anti-rabbit IgG-HRP (1:2000, Cat: HA1001-100, Huabio) and goat anti-mouse IgG-HRP (1:2000, Cat: HA1006, Huabio).

Immunofluorescence

Immunofluorescent staining was another intuitive method to assess the relative protein expression of cell lines. Cells were treated with different concentrations of BSGLWE (0, 4 mg/mL). After 24 hrs, cells were fixed with 4%

paraformaldehyde for 15 mins at room temperature. After being washed with PBS, the cells were permeabilized with 0.5% Triton X-100 at room temperature for 20 min (antigen expressed on cell membrane omits this step) and blocked with 5% BSA for 30 min, then incubated with primary antibody overnight at 4°C. The next day, secondary antibody was used at a 1:1000–2000 dilution in 5% BSA and incubated for 1 h at room temperature. The cells not incubated with primary antibody were regarded as negative controls. These cells were observed and photographed under a fluorescence microscope.

Xenograft Orthotopic Model

All experiments were performed in accordance with the guidelines of the Zhejiang University Ethics Committee and approved by the Research Ethics Committee of the Second Affiliated Hospital of Zhejiang University School of Medicine, China. Four-week-old nude mice, which were obtained from Shanghai Laboratory Animal Center of Chinese Academy of Sciences, were brought up under specific pathogen-free conditions. About 2×10^6 stable transfected HOS cells, which were transfected with luciferase (Hos-luc) for in vivo imaging, were injected into the marrow cavity of the right tibia. After 7 days, based on the results of the luminescence intensity measured by an in vivo bioluminescence imaging system, those mice with a very high or low luminescence signal were killed, and then the rest mice were randomly divided into two groups (five mice per group). Starting from the seventh day, the mice of the negative control (NC) group received daily intragastric gavage of 200 uL of PBS; The BSGLWE group received daily intragastric gavage of 600 mg/kg BSGLWE. The body weights of the mice were recorded every 3 days, and the luminescence intensity of each mouse was measured and recorded weekly. After 21 days of treatment, all mice were euthanized by chloral hydrate overdose and killed. Then, tibial tumors were excised and weighed, and fixed with 4% paraformaldehyde for further analysis.

In vivo Bioluminescence Assay

An in vivo bioluminescence assay was utilized to assess the luminescence intensity of the tumor. The tumor-bearing mice were anesthetized with isoflurane about 10 mins after intraperitoneal injection of 150 μ L of luciferin (20 mg/mL). In vivo imaging was implemented using an IVIS 200 imaging system, and the results were analyzed

with Living Image Software (Version 3.0.4, Xenogen, Hopkinton, MA, USA).

Tumor Histology

After fixation, tissues from xenograft tumors were dehydrated in a graded alcohol series of ethanol and xylene and embedded in paraffin. Next, tumor tissue was cut into sections (4 μ m) and these slices were stained with hematoxylin and eosin (H&E) before being examined under a light microscope.

In situ TUNEL Staining

A TUNEL assay (Promega, Shanghai, China) was used to evaluate apoptosis. Briefly, after deparaffinization and hydration, the sections were incubated with proteinase K (20 μ g/mL) for 30 min at 37°C. After blocked with 1% BAS, the sections were incubated with the primary antibody at room temperature for 1 h. Then, the slices were incubated with the TUNEL reaction mixture. Finally, after counterstaining the nucleus, the slices will be dehydrated and sealed, which were observed and photographed under a fluorescence microscope.

Immunohistochemistry Analysis

Briefly, paraffin-embedded sections were deparaffinized in xylene and hydrated in a gradient of ethanol concentrations. After being treated with 3% H₂O₂ for 15 min, sections were immersed in 0.01 M citrate buffer at pH 6.0 for 10 min. Then, the slices were washed by PBS for 3 times before being treated with 5% BSA for 15 min at room temperature and subsequently incubated with primary antibodies against Bcl-xl, LC3B, and P62 at 4°C overnight. The slices were incubated with secondary antibody at 37°C for 1 hr. Based on the manufacturer's instructions, the sections were stained with the enzyme substrate 3', 3'-diaminobenzidinetetrahydrochloride (DAB, Biological Technology, China) and counter-stained. Staining was scored according to the staining intensity (0-negative, 1-weak, 2-moderate, and 3-strong) and the percentage of stained cells (0: \leq 5%, 1: 6-25%, 2: 26-50%, 3: 51-75%, 4: $>$ 75%). The sections were independently measured by two pathologists and photographed under a light microscope.

Statistical Analysis

The results were described as the mean \pm standard deviation (SD). The data from groups were analyzed using a one-way ANOVA and Student's *t*-test was performed

using GraphPad Prism (v6.0). All statistics were analyzed by IBM SPSS Statistics 20.0 software (IBM, Armonk, NY, USA). Statistical significance was identified as $P < 0.05$.

Results

BSGLWE Inhibits OS Cell Proliferation in vitro

To explore the effects of BSGLWE on osteosarcoma, HOS, MG-63 and U2 cells were treated with different concentrations of BSGLWE for 24, 48 and 72 hrs. Afterward, CCK8 Kit was used to evaluate the cell viability (Figure 1A). Results showed that though low concentrations of BSGLWE had a certain proliferative effect on tumor cells, cell viability was significantly inhibited as the dose increases. Specifically, with the increase of BSGLWE from 0 to 2 mg/mL, cell viability was promoted in HOS and MG-63 cells at 24 or 48 hrs, while a light promotion was observed in U2 cells at 72 hrs. However, BSGLWE could gradually enhance its growth inhibitory potential for osteosarcoma cells in the range of 2–16 mg/mL. The IC₅₀ of BSGLWE at 24 hrs was 5.33 mg/mL for HOS cells, 3.799 mg/mL for MG-63 cells, and 4.298 mg/mL for U2 cells. Next, we chose concentrations of 2 mg/mL and 4 mg/mL BSGLWE and a time point of 24 h for the colony formation experiments. Consistent with previous conclusions, the results of colony formation confirmed that BSGLWE suppressed the proliferation of osteosarcoma cells in a dose-dependent manner (Figure 1B and C). Cell cycle analysis demonstrated significantly increased cell percentages in the G2/M phase (HOS: 4 mg/mL 16.5 \pm 0.82%; 8 mg/mL 22.78 \pm 0.73%. U2: 4 mg/mL 14.98 \pm 1.12%; 8 mg/mL 21.23 \pm 0.82%) for BSGLWE relative to those of the NC group (HOS: NC 11.42 \pm 1.02%; U2 8.9 \pm 0.47%) in the HOS and U2 cell lines, respectively (Figure 1D). These results indicated that the cell cycle progression at G2/M phase was arrested by the BSGLWE.

BSGLWE Inhibits Migration of OS Cell in vitro

Based on the reality that cell migratory behavior is the most important determinant of metastasis in tumor progression, we utilized a wound-healing assay to evaluate the anti-cancer effect of BSGLWE. Same with our expectations, BSGLWE significantly delayed the cell re-colonization into the wound area compared with control cells after 12 h in both HOS and U2 cell lines (Figure 2A and B). Then, we conducted a transwell chamber assay to verify the conclusion we drew

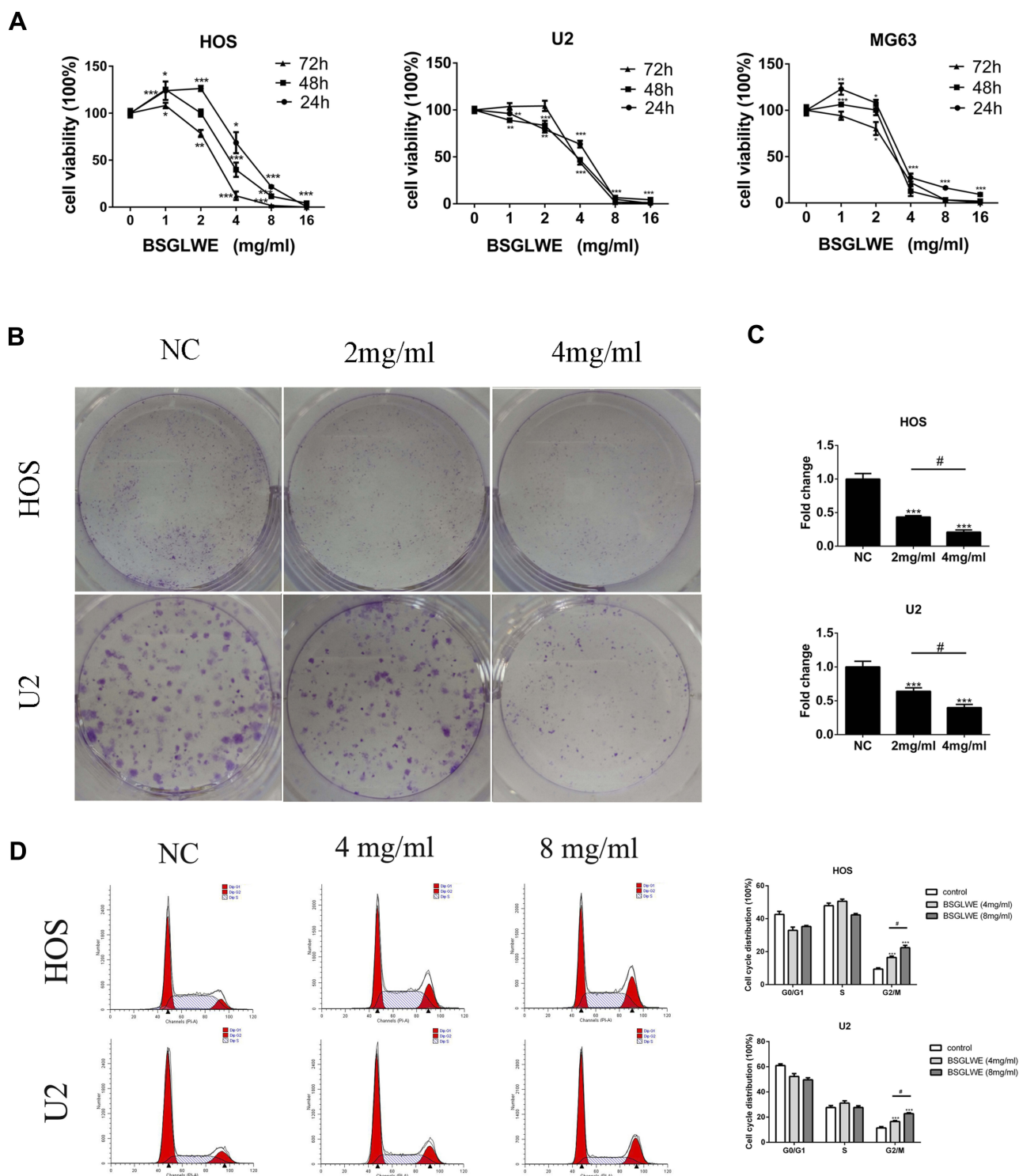


Figure 1 BSLWE inhibits osteosarcoma cell proliferation in vitro. **(A)** Three osteosarcoma cell lines were treated with different concentrations of BSLWE for 24, 48 or 72 hrs before CCK-8 assays were used. **(B, C)** BSLWE significantly inhibits colony formation compared with NC in HOS and U2 cell lines. These data were detected by a microplate reader and a microscope, respectively. **(D)** HOS and U2 cells were treated with different concentrations of BSLWE (0, 4, 8 mg/mL) for 24 hrs. Cell cycle was analyzed by flow cytometry. Error bar = mean \pm SD of at least triplicate experiments. * $P < 0.05$, ** $P < 0.01$, *** $P < 0.001$ versus control, # $P < 0.05$ versus BSLWE treatment.

from the wound-healing assay. As shown in the Figure 2C and D, BSLWE declined the ability of osteosarcoma cells to migrate compared with the control group after 8 hrs, and

the inhibitory effect of the high-dose group is more obvious (HOS: NC 498.67 ± 20.95 cells per field; 2 mg/mL 312.33 ± 21.25 cells per field; 4 mg/mL 180.67 ± 15.33 cells per field.

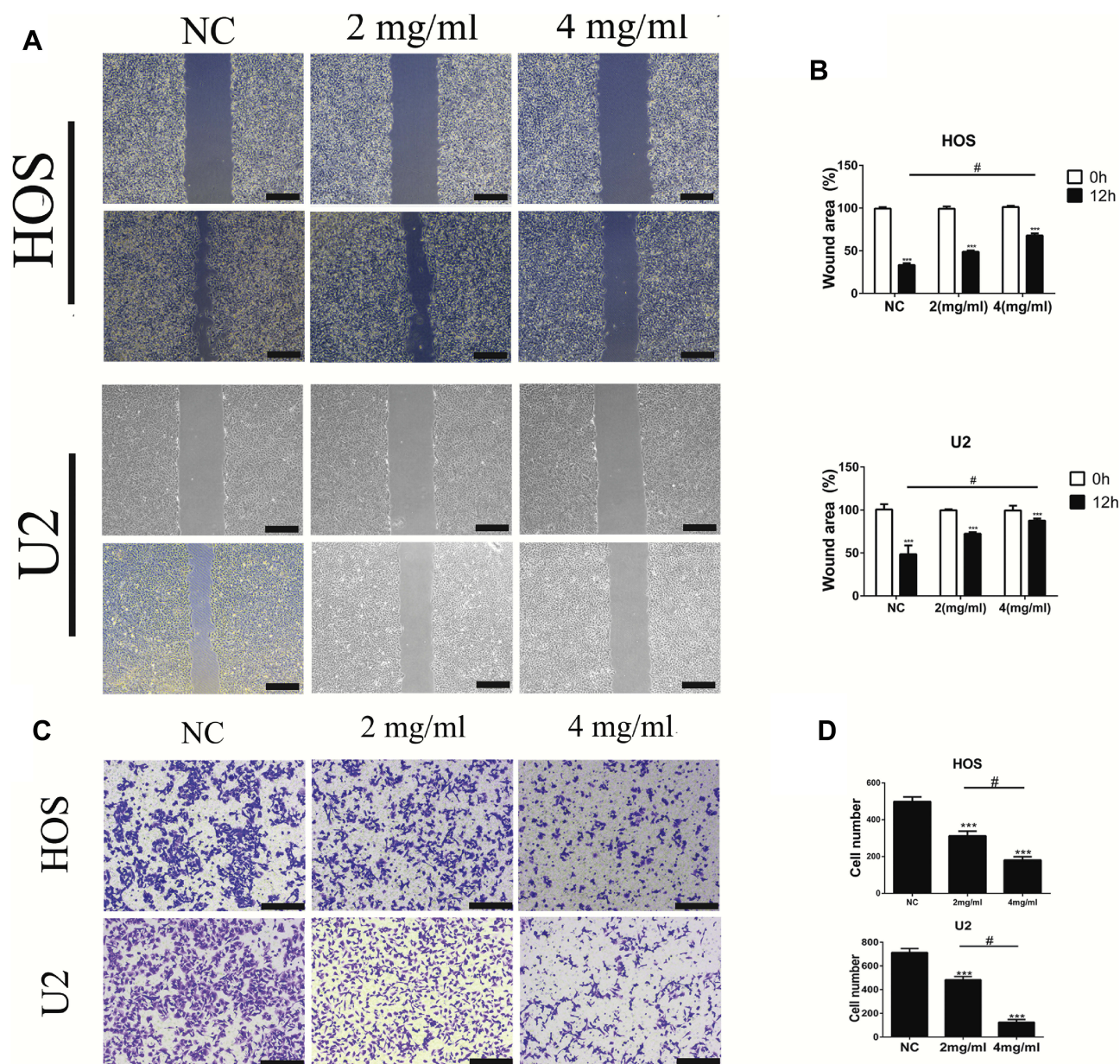


Figure 2 BSGLWE inhibits osteosarcoma cell migration in vitro. **(A, B)** The HOS and U2 osteosarcoma cell lines were incubated with BSGLWE or control for 12 hrs, and the photographs taken at 0 and 12 hrs are statistically analyzed by Image J software. The wound-healing assay showed that the percentage of wound area in the BSGLWE-treated group was higher than in the NC group. **(C, D)** The migration ability of HOS and U2 cells was significantly attenuated in the BSGLWE group relative to the NC group, which was evaluated using a transwell assay. Magnification, $\times 40$ **(A)**, $\times 100$ **(C)**. Scale bar, 500 μm **(A)**, 200 μm **(C)**. Error bar = mean \pm SD of at least triplicate experiments. *** $P < 0.001$ versus control, # $P < 0.05$ versus BSGLWE treatment. Each assay was repeated 3 times.

U2: NC 713.33 ± 27.08 cells per field; 2 mg/mL 482 ± 23.37 cells per field; 4 mg/mL 124.67 ± 19.01 cells per field). These data illustrated that BSGLWE suppressed the migration of osteosarcoma cells in a dose-dependent manner.

BSGLWE Induces Caspase-Dependent Apoptosis of OS Cell in vitro

According to the previous studies about *G. lucidum*, acceleration of apoptosis is the most crucial mechanism in inducing

tumor cell death.^{9,18,19} Thus, we carried out Hoechst 33342 staining to assess whether apoptosis was responsible for BSGLWE-induced cell death. The pictures of the changes of morphological alterations in the apoptotic cells were taken by the fluorescence microscope (Figure 3A). It was apparent that there were more chromatin condensation and apoptotic bodies in the BSGLWE-treated group (4 mg/mL and 8 mg/mL) compared with the NC group (Figure 3B). In addition, the ability of BSGLWE in inducing apoptosis was verified with

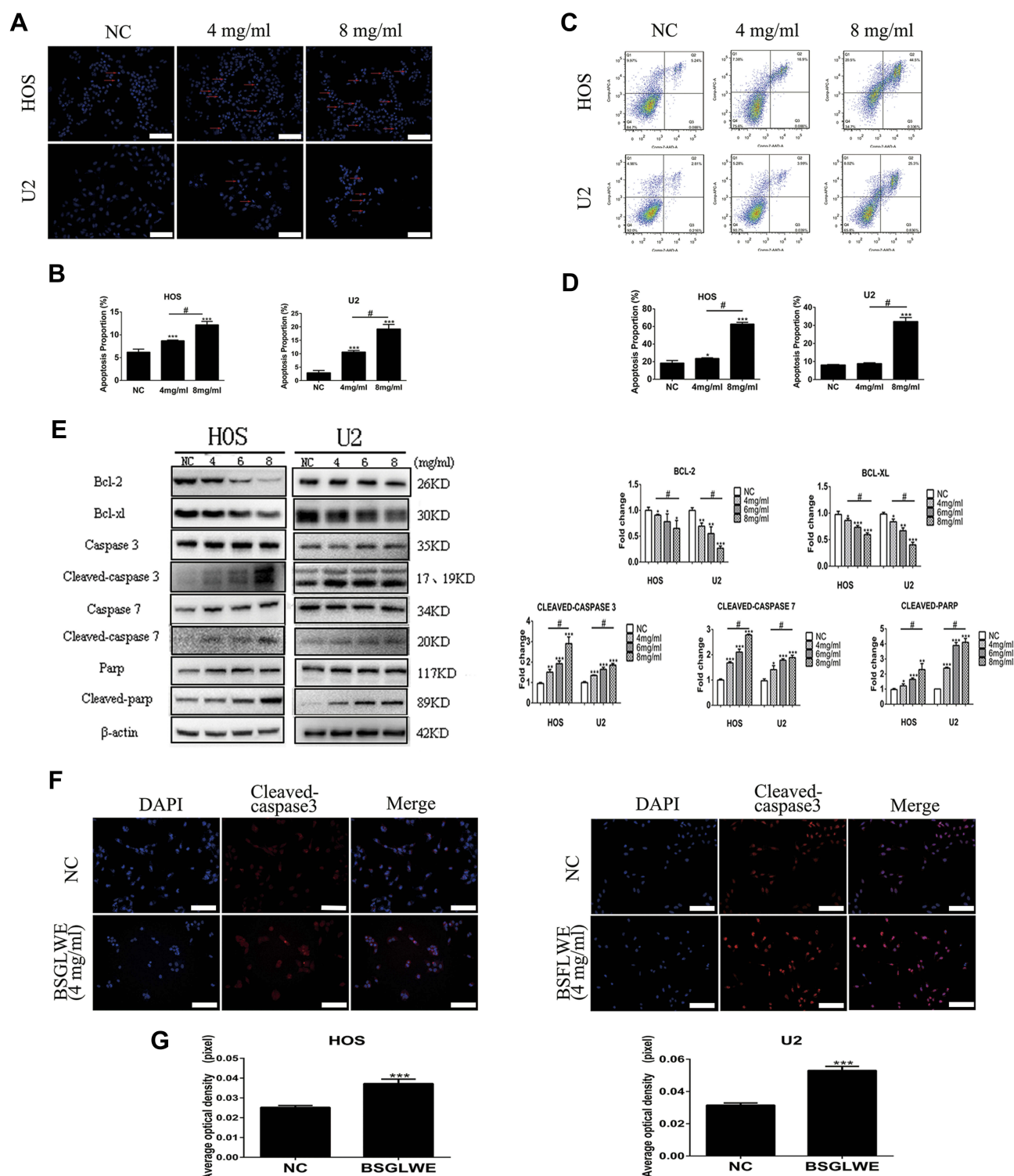


Figure 3 BSLWE induces caspase-dependent apoptosis of OS cell in vitro. **(A, B)** Hoechst 33342 staining showed that the percentage of apoptotic cells in the BSLWE group was higher than in the NC group. The red arrows mean apoptotic bodies and nuclear condensation. **(C, D)** After staining with an Annexin V-APC/7-AAD kit, the differently treated cells were analyzed by flow cytometry. The results indicated that the percent of total apoptotic cells significantly increased in the BSLWE-treated group. **(E)** The expression of the following apoptosis-related proteins was determined by Western blot analysis: cleaved PARP, caspase-3, -7, and Bcl-2 family members Bcl-2, Bcl-xl. **(F, G)** The HOS and U2 osteosarcoma cell lines were incubated with BSLWE (4mg/mL) or control for 24 hrs. The expression level of the protein cleaved-caspase 3 was significantly increased in HOS and U2 cell lines after BSLWE treatment detected using immunofluorescence assays. Each assay was repeated 3 times. Magnification, $\times 200$ **(A)**, $\times 200$ **(F)**. Scale bar, 100 μ m **(A)**, 100 μ m **(F)**. Error bar = mean \pm SD of at least triplicate experiments. * $P < 0.05$, ** $P < 0.01$, *** $P < 0.001$ versus control, # $P < 0.05$ versus BSLWE treatment.

flow cytometry analysis (Figure 3C and D). Annexin V-APC/7-AAD kit results further demonstrated that BSLWE induced apoptosis of osteosarcoma cell lines. In terms of data, the rate of apoptotic cells in BSLWE group (HOS: 4 mg/mL 23.69±0.71%; 8 mg/mL 62.80±1.93%, $P < 0.05$. U2: 4 mg/mL 8.86±0.42%; 8 mg/mL: 32.14±2.20%, $P < 0.05$) was significantly higher than the percentage in control group (HOS: 18.41±2.97%; U2: 8.08±0.27%, $P < 0.05$). As shown in Figure 4A, apoptotic chromatin condensation and apoptotic bodies (yellow arrow in picture) were clearly observed.

Overall, these results confirmed that BSLWE induced apoptosis of osteosarcoma cells.

A Western blot was executed to examine the apoptosis-related protein expression, so that we could explore the underlying mechanisms of pro-apoptotic effects induced by BSLWE. As shown in Figure 3E, in the HOS cell line, the protein expression of cleaved caspase-3, -7, and poly(ADP ribose) polymerase (PARP) were upregulated evidently compared with NC group after treating with 8 mg/mL BSLWE but Bcl-2 and Bcl-xl were downregulated. We also get the

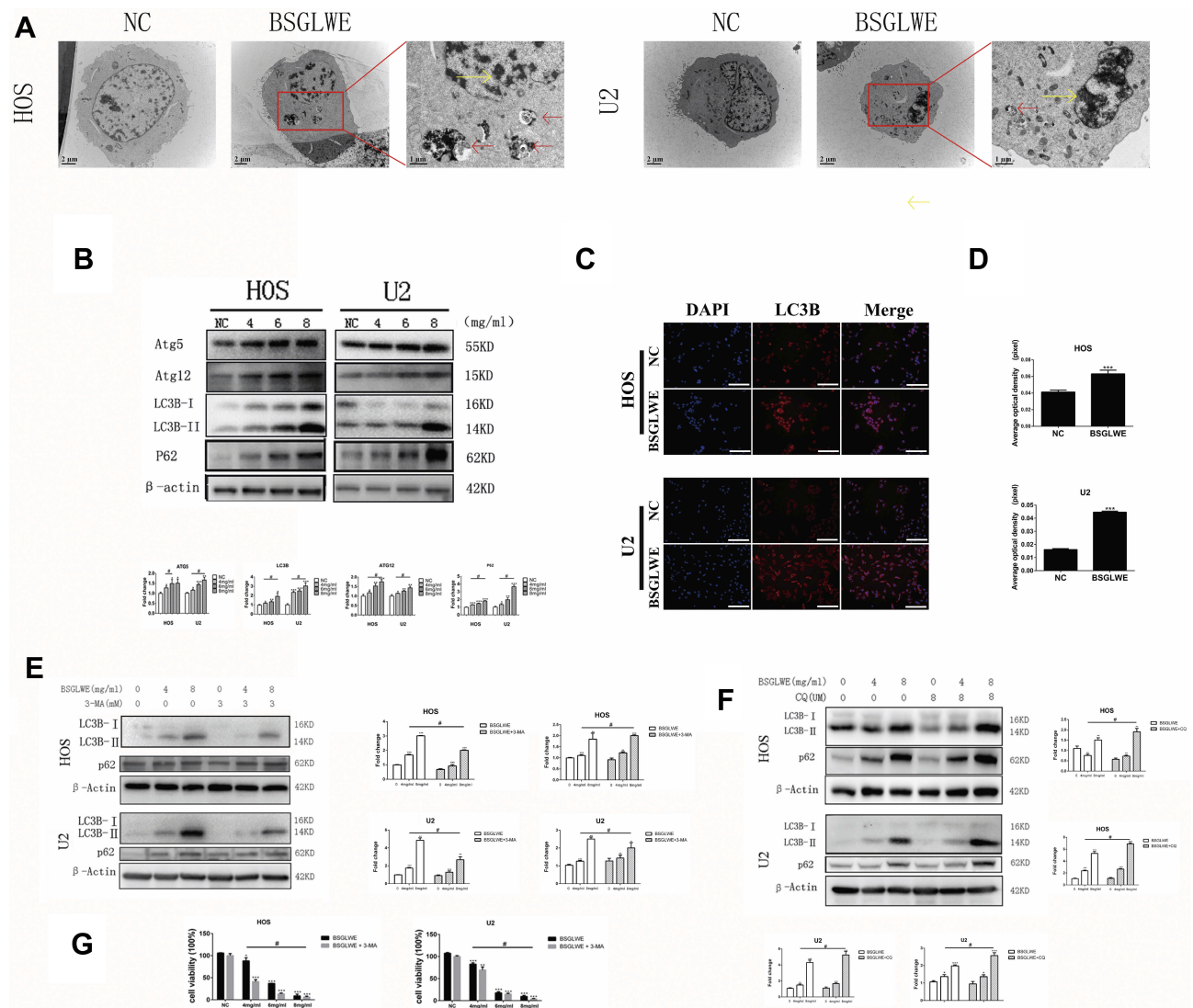


Figure 4 BSLWE restricts autophagic flux of OS cells in vitro. (A) Morphological changes induced by BSLWE were observed by transmission electron microscopy. BSLWE group cells were treated with BSLWE (4mg/mL). The yellow arrows mean apoptotic bodies and nuclear condensation. The red arrows mean autophagosomes. Scale bar, 2 μ m. (B) The HOS and U2 osteosarcoma cells were treated with different concentrations of BSLWE for 24 h. The expression of those autophagy-related proteins, which included ATG5, ATG12, LC3B, P62, was measured by a Western blot assay. (C, D) An immunofluorescence assay revealed the level of protein LC3B increased in the BSLWE (4mg/mL) group compared with the NC group in both HOS and U2 cell lines. (E) HOS and U2 cells were treated with different concentrations of BSLWE (0,4,8 mg/mL), with or without 3-MA (3mM), (F) or with or without CQ (8 μ M) for 24 h. The protein expressions of LC3B and p62 were measured by Western blotting. (G) HOS and U2 cells were treated with different concentrations of BSLWE (0,4,6,8 mg/mL), with or without 3-MA (3mM). CCK-8 assay was used to test cell viability. Each assay was repeated 3 times. Magnification, $\times 200$ (C). Scale bar, 100 μ m (C). Error bar = mean \pm SD. * $P < 0.05$, ** $P < 0.01$, *** $P < 0.001$ versus control, # $P < 0.05$ versus BSLWE treatment.

same tendency in the U2 cell line. Immuno-fluorescence was considered to be an effective method to examine the relative expression intensity of the apoptosis-related protein in the BSGLWE (4 mg/mL) and the NC group. Manifestly, the fluorescence intensity of cleaved-caspase-3 protein was much more in BSGLWE (4 mg/mL) group than the control group (Figure 3F and G). These results indicated that BSGLWE induced caspase-dependent apoptosis of osteosarcoma cells in vitro.

BSGLWE Restricts Autophagic Flux in OS Cell

In many cases, autophagy and apoptosis can be triggered simultaneously in the same cell by common upstream signals.¹² Apoptotic bodies and autophagosomes were clearly found in TEM results. Not surprisingly, we speculated autophagy played a critical role in BSGLWE-induced tumor cell death. More than 20 autophagy-associated gene (ATG) family proteins are involved, and the well-known LC3 (microtubule-associated protein light chain 3) belongs to the ATG8 family.¹⁵ In the beginning, it is pro-LC3, immediately its C-terminus is hydrolyzed by ATG4 to cleave a piece of polypeptide, turning into LC3-I. During autophagy, LC3-I is covalently bound to phosphatidylethanolamine under the action of ATG5-ATG12 complex to form LC3-II, which binds to the autophagosome membrane.^{20,21} Thus, the magnitude of the LC3-II/I ratio can estimate the level of autophagosome. There are three types of LC3 in mammals, LC3A, LC3B, and LC3C. LC3B is the most studied family protein and is used to monitor autophagic activity.

We used TEM and the two experimental methods mentioned in detecting apoptosis-related protein expression: Western blot and immunofluorescence. While observing apoptosis by TEM, we also clearly observed the formation of autophagosomes (Figure 4A, red arrow). As illustrated in Figure 4B, the intensity of the LC3B-II band and the expression of the ATG5, ATG12 protein were markedly enhanced upon BSGLWE treatment in a dose-dependent manner compared with the untreated groups. This result was further verified by the immunofluorescence staining (Figure 4C and D). However, in Figure 4A, we found that BSGLWE increased p62 levels in a dose-dependent manner. P62 is regarded as the substrate of autophagic degradation and has a negative correlation with autophagy. These results showed us that BSGLWE led to autophagosome accumulation by impairing autophagic degradation.

We further validated the above conclusions by two different autophagy inhibitors, early-stage inhibitor 3-MA and late-stage inhibitor CQ. In Figure 4E, although the presence of 3-MA reduced the expression of LC3B-II in the absence of BSGLWE, the BSGLWE group significantly increased the expression of LC3B-II and p62 in a dose-dependent manner. What's more, the presence of CQ further enhanced BSGLWE-induced accumulation of LC3B-II and p62, indicating synergistic inhibition of autophagy flux (Figure 4F). As shown in Figure 4G, CCK-8 assay showed that inhibition of autophagosome formation by 3-MA exacerbated BSGLWE-induced cell death. These data suggest that BSGLWE blocked autophagic flux by inducing initiation of autophagy and increasing autophagosome accumulation of osteosarcoma cells.

BSGLWE Inhibits Osteosarcoma in vivo

In vitro studies have proved that BSGLWE suppressed osteosarcoma cell proliferation and migration, as well as promoted cell apoptosis and blocked autophagic flux. We further examined the in vivo effects of BSGLWE. A commonly used orthotopic modeling method is that HOS stably transfected cells were inoculated into the tibia of nude mice. As shown in Figure 5A, tumor size was calculated based on luminescence intensity, and the luminescence intensity of the control group was markedly higher than the BSGLWE-treated group. The physical photos of these excised tibia tumors and corresponding volume and weight charts (Figure 5B and C) indicated that there was a difference in tumor sizes and weights between the two groups after 21 days; the data showed that the BSGLWE significantly inhibited tumor growth in vivo. The excised tumor specimens were used for further pathological analysis. The terminal deoxynucleotidyl transferase-mediated (d)-UTP nick-end labeling (TUNEL) assays and Hematoxylin and eosin (H&E) staining revealed more tumor cell death in BSGLWE group (Figure 5D). Immunohistochemical quantitative analysis confirmed that the expression level of Bcl-xl was lower in the BSGLWE group than in the NC group, which meant that BSGLWE could induce osteosarcoma apoptosis in vivo. Furthermore, the expression levels of LC3B and P62 revealed that BSGLWE also restricted the autophagic flux of osteosarcoma in vivo. What's more, as shown in Figure 5E, H&E staining indicated that no obvious toxic effects had been observed in mice, including heart, liver, spleen, lung and kidney. These results clearly demonstrated that BSGLWE not only inhibited the growth of

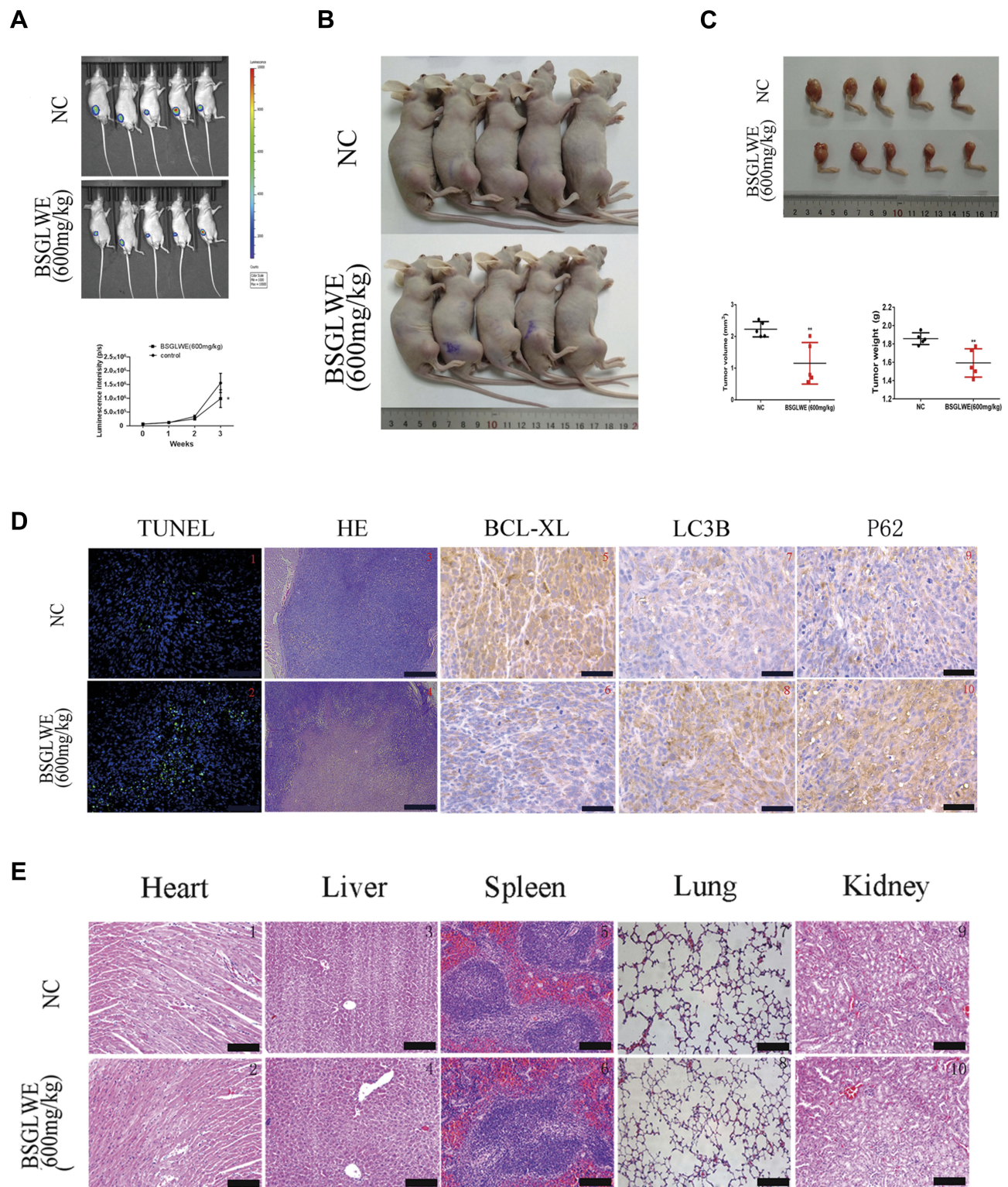


Figure 5 BSGLWE inhibits osteosarcoma growth in vivo. **(A)** After 21 days of BSGLWE treatment, luciferase intensity of tumor was measured and calculated by an in vivo imaging system. **(B, C)** The photographs show tumor formation in two groups. There was a significant difference in tumor sizes and weights between the two groups after 21 days. **(D)** TUNEL assays were utilized to assess the apoptotic status of tumor tissues. BSGLWE promoted extensive tumor cell necrosis was proved by H&E staining. The levels of BCL-XL, LC3B and P62 were further examined by immunohistochemistry. **(E)** There were no obvious toxic effects observed in the important organs of the experimental mice between the BSGLWE-treated group and the control group. Error bar = mean \pm SEM. Magnification, $\times 200$ (d1–2), $\times 40$ (d3–4, e1–10), $\times 400$ (d5–10). Scale bar, 100 μ m (d1–2), 500 μ m (d3–4, e1–10), 50 μ m (d5–10). Error bar = mean \pm SD. * $P < 0.05$, ** $P < 0.01$.

osteosarcoma, but also induced apoptosis and blocked autophagy in vivo.

Discussion

Osteosarcoma is a malignant bone tumor with high incidence in adolescents for the reason that it usually develops in growing bones, and most lesions are located in the lower end of the femur and the upper end of the tibia.^{1,22} As a result of its high rate of the propensity for local invasion and rapidly metastasizes, the prognosis of patients with osteosarcoma is poor.²³ In currently, surgery and combination chemotherapy is a common method for the treatment of primary osteosarcoma. Notwithstanding the great progress that has been made in recent years, a 5-year survival rate of osteosarcoma patients with metastases was nearly 20%.²⁴ Besides, chemotherapeutics have many side effects, such as neutropenia, thrombocytopenia, anemia, hair loss and a series of adverse reactions.²⁵ Thus, an innovative drug that has less side effects and higher potency is urgently needed. *G. lucidum* was regarded as an effective anticancer drug in the treatment of many kinds of tumors. In our study, we discovered that BSGLWE promoted osteosarcoma cell death in vitro and inhibited osteosarcoma growth in vivo. What's more, our results suggested apoptosis and autophagy of osteosarcoma were induced by BSGLWE.

In recent years, more studies of traditional Chinese medicines about their application in the prevention and treatment of cancer have emerged.²⁶ One of the most widely used traditional Chinese medicines is *G. lucidum*, which has been considered as a natural medicine to improve the body's immune function and promote longevity. *G. lucidum* has been used for the treatment of various human diseases, such as hyperglycemia, inflammation and cancer.^{8,27} Nowadays, we have a deeper understanding of it that the major bioactive natural components of *G. lucidum* are polysaccharides and triterpenes.²⁸ GLPs were proved significantly suppressed tumorigenesis, by hindering proliferation, inducing cell cycle arrest and apoptosis, immunomodulation, inhibiting angiogenesis and invasion. BSGLWE was confirmed to mainly contain GLPs, giving it antitumor function. The previous research indicated that BSGLWE inhibited colorectal cancer carcinogenesis by suppressing cell proliferation, inducing cell cycle arrest and cell apoptosis.⁹ However, the effects of the BSGLWE effect on human osteosarcoma and its underlying mechanisms have not been reported. In our study, we demonstrated that BSGLWE had similar anticancer effects on osteosarcoma. From the data of CCK-8 kit, which was commonly

utilized to describe cell proliferation, we drew a conclusion that BSGLWE had an inhibition effect on osteosarcoma cells in vitro. Precisely, in the range of 2–16 mg/mL, BSGLWE suppressed cell proliferation in a dose-dependent manner. In this experiment, low concentrations of BSGLWE, specifically 0–2 mg/mL, promoted the proliferation of osteosarcoma cells, which was consistent with previous research results.²⁹ Then, colony formation assay was used to further confirm what we had obtained. In the beginning, we used a concentration of 4 mg/mL and 8 mg/mL for the clone formation experiment, but the results showed that all the cells died at the 8 mg/mL concentration on the next day. Therefore, after conducting the pre-experimental exploration conditions, we chose 2 mg/mL and 4 mg/mL as the experimental concentration, and we got the same conclusion that BSGLWE inhibited cell proliferation in a dose-dependent manner. In addition, with cell cycle flow cytometry assays, we confirmed that BSGLWE could block cell cycle progression at G2/M phase, which was consistent with previous reports. Cell migration is the most important determinant of metastasis in tumor progression, and those unregulated cell migration leads to metastasis and recurrence, ultimately resulting in poor prognosis.³⁰ Therefore, we as well as testified the repression ability of BSGLWE on the migration of osteosarcoma cells in vitro by wound-healing assay and transwell chamber assay. After 12 h, the wound area percentages of HOS and U2 cells in the control group were markedly lower than BSGLWE groups, and the high-dose BSGLWE group showed better inhibition of cell migration. A transwell chamber assay showed that the number of cells on the lower membrane in the BSGLWE 4 mg/mL group was significantly decreased than the NC group. These data indicated that BSGLWE acts as an inducer for migration inhibition in vitro and it may be a potential drug that inhibits tumor metastasis.

Apoptosis serves a key role in drug-induced cell death and plays critical functions to inhibits cancer development and progression.³¹ In our study, we found that BSGLWE-induced cell death by activating cell apoptosis detected by Hoechst 33342 staining assay and Annexin V-APC/7-AAD kit. In the HOS cell line, the apoptosis percentage of 8 mg/mL group is 62.80%, which is significantly higher than 18.4% in the control group. The U2 cell apoptosis percentage of 8 mg/mL group is 32.14%, which is 4 times greater than the apoptosis percentage in the control group. To prove this result is reliable, we performed a TEM to observe whether the cells after BSGLWE treatment showed apoptosis-specific morphological changes. Significant apoptotic bodies and nuclear lysis in cells treated with BSGLWE. These data certified that BSGLWE induced apoptosis of osteosarcoma cells. Studies demonstrate

that there are two main apoptotic pathways: the extrinsic or death receptor pathway and the intrinsic or mitochondrial pathway, and these pathways can interact with each other through certain proteins.³² However, the extrinsic and intrinsic converge on the same terminal pathway, which is initiated by the cleavage of caspase-3.¹² Many studies about *G. lucidum* have shown that the antitumor effect of *G. lucidum* is achieved by stimulating the apoptotic pathway.^{9,11,19} Consistent with their conclusions, we observed that BSGLWE activated caspase-dependent apoptosis, as well as down-regulated the expression of the antiapoptotic proteins Bcl-2 and Bcl-xl. Caspase-3, caspase-6, and caspase-7 serve as executioner caspases, which is activated by any of the initiator caspases (caspase-8, caspase-9, or caspase-10) to cleaving various substrates. In our study, we found that the expression level of cleaved-caspase3, cleaved-caspase7 and cleaved-PARP was increased. Overall, these results illustrated that BSGLWE induced caspase-dependent apoptosis to prompted osteosarcoma cell death.

Interestingly, when we measured apoptosis by TEM, the formation of autophagosomes was clearly observed. At present, autophagy plays a dual role in cancer, acting as both tumor-inhibitor and tumor promoter, which depends on the cell and tissue types and the stages of the tumor.³³ In some cases, autophagy can help cell survival; and in other cases, it can lead to cell death.¹² Coincidentally, the effects of *G. lucidum* on autophagy of tumor cells were paradoxical. *G. lucidum* ribonuclease was detected to suppress cell autophagy in colorectal cancer cells.³⁴ On the contrary, the methanolic extract of *G. lucidum* induces autophagy of gastric adenocarcinoma cells.³⁴ In this study, we found that BSGLWE induced autophagosome formation by the results of TEM, Western blot and immunofluorescence. The formation of autophagosome is only one aspect of assessing autophagy activity, and degradation of autophagy substrates needs to be detected. However, we accidentally discovered that the expression of P62 was markedly enhanced by BSGLWE. This indicated that BSGLWE could facilitate autophagy initiation and inhibit the autophagic degradation of osteosarcoma cells. Then, we explore the effects of autophagy inhibitor 3-MA and CQ on BAGLWE-induced LC3B-II and p62 accumulation. As expected, 3-MA reduced the expression of LC3B-II and increased the expression of P62. Because 3-MA is an autophagosome-forming inhibitor, the expression of LC3B should be low in those groups with 3-MA. However, we were surprised to find that the LC3B protein expression in the BSGLWE (8mg/mL) group was still

high, which reminded us of that BSGLWE could antagonize the action of 3-MA through other pathways to promote the formation of autophagosomes. This interesting phenomenon needs to be explored further. Additionally, the expressions of LC3B-II and P62 in CQ combined with the BSGLWE group were higher than the CQ group or BSGLWE group implied a synergistic effect of BSGLWE on inducing autophagic autophagosome accumulation. What's more, CCK-8 assay showed that inhibition of autophagosome formation by 3-MA exacerbated cell death induced by BSGLWE, suggesting synergistic inhibition of autophagic flux. Our results demonstrated that BSGLWE blocked autophagic flux by inducing initiation of autophagy and increasing autophagosome accumulation of osteosarcoma cells.

It was reported previously that *G. lucidum* treatment led to inhibition of various tumors in vivo.^{10,35} In addition, the BSGLWE was examined that it could significantly inhibit colorectal cancer cell proliferation and tumor growth.⁹ Emerging research suggests that because natural compounds can alter the differentiation state of selected cell types, more effective treatments may be achieved in the future based on the type and genetic phenotype of the cancer.³⁶ However, inducing cell apoptosis and blocking autophagic flux to promote tumor cell necrosis is the most important mechanism of antitumor drugs.³¹ In our study, we proved that BSGLWE inhibited osteosarcoma growth by inducing cell apoptosis and restricting autophagy activity after a 3-week treatment. The tumor sizes and weights of the BSGLWE-treated group were significantly lower than the control group. Moreover, during our daily experiment, we did not observe abnormal behavior (loss of appetite, hematochezia, lethargy, etc.) in the experimental group and no obvious toxic effects had been observed in the important organs, which reflected that BSGLWE had no obvious side effects. These results indicated that the BSGLWE might be a promising drug, for the reason that BSGLWE could inhibit osteosarcoma growth and no obvious toxic effects had been observed.

HOS, MG-63, U-2 OS and Saos-2 cell lines were very representative in osteosarcoma and used commonly in previous studies. HOS, SAOS-2, and MG63 are osteosarcoma cell lines with p53 mutations, while U2-OS is a p53-wt cell line.^{37,38} Due to the limitations of time and budget, we selected two representative cells (HOS and U2-OS) for subsequent experiments. *Ganoderma lucidum*, containing a variety of active ingredients, has different targets, which

leads to the activation or inhibition of various signaling pathways in cells, thus increasing the difficulty of signaling pathway exploration. In our next study, we will extract effective monomers from *Ganoderma lucidum* to explore the complete potential signaling pathways involved in its inhibitory effects on osteosarcoma.

Conclusions

In conclusion, BSLWE can inhibit osteosarcoma proliferation and migration, and also induce apoptosis and block autophagic flux. Moreover, BSLWE exhibited potent antitumor activity and no obviously significant side effects in vivo. Our results provide a potential direction for the application of *G. lucidum*. Further studies are required to investigate complete potential signaling pathways.

Data Sharing Statement

The data used to support the findings of this study are available from the corresponding author upon request.

Acknowledgments

This study was supported by grants from the National Natural Science Foundation of China (No. 31771106, No.81772325).

Author Contributions

All authors contributed to data analysis, drafting or revising the article, gave final approval of the version to be published, and agree to be accountable for all aspects of the work.

Disclosure

The authors declare that they have no conflicts of interest in this work.

References

- Rivera-Valentin RK, Zhu L, Hughes DPM. Bone sarcomas in pediatrics: progress in our understanding of tumor biology and implications for therapy. *Paediatr Drugs*. 2015;17(4):257–271. doi:10.1007/s40272-015-0134-4
- Morrow JJ, Khanna C. Osteosarcoma genetics and epigenetics: emerging biology and candidate therapies. *Crit Rev Oncog*. 2015;20(3–4):173–197. doi:10.1615/CritRevOncog.v20.i3-4
- Tan ML, Choong PF, Dass CR. Osteosarcoma: conventional treatment vs. gene therapy. *Cancer Biol Ther*. 2009;8(2):106–117. doi:10.4161/cbt.8.2.7385
- Xu Z, Chen X, Zhong Z, Chen L, Wang Y. *Ganoderma lucidum* polysaccharides: immunomodulation and potential anti-tumor activities. *Am J Chin Med*. 2011;39(1):15–27. doi:10.1142/S0192415X11008610
- Jin H, Jin F, Jin JX, et al. Protective effects of *Ganoderma lucidum* spore on cadmium hepatotoxicity in mice. *Food Chem Toxicol*. 2013;52:171–175. doi:10.1016/j.fct.2012.05.040
- Lu J, Sun LX, Lin ZB, et al. Antagonism by *Ganoderma lucidum* polysaccharides against the suppression by culture supernatants of B16F10 melanoma cells on macrophage. *Phytother Res*. 2014;28(2):200–206. doi:10.1002/ptr.4980
- Chen Y, Lv J, Li K, et al. Sporoderm-broken spores of *Ganoderma lucidum* inhibit the growth of lung cancer: involvement of the Akt/mTOR signaling pathway. *Nutr Cancer*. 2016;68(7):1151–1160. doi:10.1080/01635581.2016.1208832
- Jin X, Ruiz Beguerie J, Sze DM, Chan GC. *Ganoderma lucidum* (Reishi mushroom) for cancer treatment. *Cochrane Database Syst Rev*. 2016;4:CD007731.
- Na K, Li K, Sang T, Wu K, Wang Y, Wang X. Anticarcinogenic effects of water extract of sporoderm-broken spores of *Ganoderma lucidum* on colorectal cancer in vitro and in vivo. *Int J Oncol*. 2017;50(5):1541–1554. doi:10.3892/ijo.2017.3939
- Yuen JWM, Mak DSY, Chan ES, Gohel MDI, Ng CF. Tumor inhibitory effects of intravesical *Ganoderma lucidum* instillation in the syngeneic orthotopic MB49/C57 bladder cancer mice model. *J Ethnopharmacol*. 2018;223:113–121. doi:10.1016/j.jep.2018.05.020
- Li K, Na K, Sang T, Wu K, Wang Y, Wang X. The ethanol extracts of sporoderm-broken spores of *Ganoderma lucidum* inhibit colorectal cancer in vitro and in vivo. *Oncol Rep*. 2017;38(5):2803–2813. doi:10.3892/or.2017.6010
- Marino G, Niso-Santano M, Baehrecke EH, Kroemer G. Self-consumption: the interplay of autophagy and apoptosis. *Nat Rev Mol Cell Biol*. 2014;15(2):81–94. doi:10.1038/nrm3735
- Yang Z, Klionsky DJ. Mammalian autophagy: core molecular machinery and signaling regulation. *Curr Opin Cell Biol*. 2010;22(2):124–131. doi:10.1016/j.ceb.2009.11.014
- Boya P, Gonzalez-Polo RA, Casares N, et al. Inhibition of macroautophagy triggers apoptosis. *Mol Cell Biol*. 2005;25(3):1025–1040. doi:10.1128/MCB.25.3.1025-1040.2005
- Kondo Y, Kanzawa T, Sawaya R, Kondo S. The role of autophagy in cancer development and response to therapy. *Nat Rev Cancer*. 2005;5(9):726–734. doi:10.1038/nrc1692
- Kroemer G, Levine B. Autophagic cell death: the story of a misnomer. *Nat Rev Mol Cell Biol*. 2008;9(12):1004–1010. doi:10.1038/nrm2529
- Cerezo M, Rocchi S. New anti-cancer molecules targeting HSPA5/BIP to induce endoplasmic reticulum stress, autophagy and apoptosis. *Autophagy*. 2017;13(1):216–217. doi:10.1080/15548627.2016.1246107
- Dai J, Xu LJ, Han GD, et al. Down-regulation of long non-coding RNA ITGB2-AS1 inhibits osteosarcoma proliferation and metastasis by repressing Wnt/beta-catenin signalling and predicts favourable prognosis. *Artif Cells Nanomed Biotechnol*. 2018;46:1–8.
- Zheng L, Wong YS, Shao M, Huang S, Wang F, Chen J. Apoptosis induced by 9,11dehydroergosterol peroxide from *Ganoderma lucidum* mycelium in human malignant melanoma cells is McI1 dependent. *Mol Med Rep*. 2018;18(1):938–944. doi:10.3892/mmr.2018.9035
- Wang X, Qi H, Wang Q, et al. FGFR3/fibroblast growth factor receptor 3 inhibits autophagy through decreasing the ATG12-ATG5 conjugate, leading to the delay of cartilage development in achondroplasia. *Autophagy*. 2015;11(11):1998–2013. doi:10.1080/15548627.2015.1091551
- Frankel LB, Lubas M, Lund AH. Emerging connections between RNA and autophagy. *Autophagy*. 2017;13(1):3–23. doi:10.1080/15548627.2016.1222992
- Geller DS, Gorlick R. Osteosarcoma: a review of diagnosis, management, and treatment strategies. *Clin Adv Hematol Oncol*. 2010;8(10):705–718.
- Anderson ME. Update on Survival in Osteosarcoma. *Orthop Clin North Am*. 2016;47(1):283–292. doi:10.1016/j.ocl.2015.08.022

24. Meyers PA, Healey JH, Chou AJ, et al. Addition of pamidronate to chemotherapy for the treatment of osteosarcoma. *Cancer*. 2011;117(8):1736–1744. doi:10.1002/cncr.25744
25. Vos HI, Coenen MJ, Guchelaar HJ, Te Loo DM. The role of pharmacogenetics in the treatment of osteosarcoma. *Drug Discov Today*. 2016;21(11):1775–1786. doi:10.1016/j.drudis.2016.06.022
26. Parekh HS, Liu G, Wei MQ. A new dawn for the use of traditional Chinese medicine in cancer therapy. *Mol Cancer*. 2009;8:21. doi:10.1186/1476-4598-8-21
27. Lin ZB. Cellular and molecular mechanisms of immuno-modulation by *Ganoderma lucidum*. *J Pharmacol Sci*. 2005;99(2):144–153. doi:10.1254/jphs.CRJ05008X
28. Ruan W, Wei Y, Popovich DG. Distinct responses of cytotoxic *Ganoderma lucidum* triterpenoids in human carcinoma cells. *Phytother Res*. 2015;29(11):1744–1752. doi:10.1002/ptr.v29.11
29. Hsieh TC, Wu JM. Suppression of proliferation and oxidative stress by extracts of *Ganoderma lucidum* in the ovarian cancer cell line OVCAR-3. *Int J Mol Med*. 2011;28(6):1065–1069. doi:10.3892/ijmm.2011.788
30. Condeelis J, Pollard JW. Macrophages: obligate partners for tumor cell migration, invasion, and metastasis. *Cell*. 2006;124(2):263–266. doi:10.1016/j.cell.2006.01.007
31. Surh YJ. Cancer chemoprevention with dietary phytochemicals. *Nat Rev Cancer*. 2003;3(10):768–780. doi:10.1038/nrc1189
32. Elmore S. Apoptosis: a review of programmed cell death. *Toxicol Pathol*. 2007;35(4):495–516. doi:10.1080/01926230701320337
33. Jiang GM, Tan Y, Wang H, et al. The relationship between autophagy and the immune system and its applications for tumor immunotherapy. *Mol Cancer*. 2019;18(1):17. doi:10.1186/s12943-019-0944-z
34. Dan X, Liu W, Wong JH, Ng TB. A ribonuclease isolated from wild *ganoderma lucidum* suppressed autophagy and triggered apoptosis in colorectal cancer cells. *Front Pharmacol*. 2016;7:217. doi:10.3389/fphar.2016.00217
35. Smina TP, Nitha B, Devasagayam TP, Janardhanan KK. *Ganoderma lucidum* total triterpenes induce apoptosis in MCF-7 cells and attenuate DMBA induced mammary and skin carcinomas in experimental animals. *Mutat Res*. 2017;813:45–51. doi:10.1016/j.mrgentox.2016.11.010
36. Diederich M, Cerella C. Non-canonical programmed cell death mechanisms triggered by natural compounds. *Semin Cancer Biol*. 2016;40-41:4–34. doi:10.1016/j.semcancer.2016.06.001
37. Chandar N, Billig B, McMaster J, Novak J. Inactivation of p53 gene in human and murine osteosarcoma cells. *Br J Cancer*. 1992;65(2):208–214. doi:10.1038/bjc.1992.43
38. Jin W, Zhou L, Yan B, et al. Theabrownin triggers DNA damage to suppress human osteosarcoma U2OS cells by activating p53 signaling pathway. *J Cell Mol Med*. 2018;22(9):4423–4436.

OncoTargets and Therapy

Publish your work in this journal

OncoTargets and Therapy is an international, peer-reviewed, open access journal focusing on the pathological basis of all cancers, potential targets for therapy and treatment protocols employed to improve the management of cancer patients. The journal also focuses on the impact of management programs and new therapeutic

agents and protocols on patient perspectives such as quality of life, adherence and satisfaction. The manuscript management system is completely online and includes a very quick and fair peer-review system, which is all easy to use. Visit <http://www.dovepress.com/testimonials.php> to read real quotes from published authors.

Submit your manuscript here: <https://www.dovepress.com/oncotargets-and-therapy-journal>

Dovepress